DEVELOPMENT OF FORMING LIMIT DIAGRAMS FOR DRY FABRICS

Chandra Kishore Reddy Emani, P. K. Mallick
Department of Mechanical Engineering, University of Michigan-Dearborn, MI 48128

Abstract

Fabric-reinforced polymer composites are being considered for many structural automotive applications because of their weight saving potential, high structural performance, and design flexibility. The manufacturing process for making these composite parts starts with making a preform of dry fabrics if a thermosetting polymer is used as the matrix or with press forming operation if a thermoplastic polymer is used as the matrix. During the press forming operation, the fabric is subjected to a complex set of deformations involving shear, tension and bending. The limits of the press forming operation are determined by the ability to produce and retain the shape of the preform without developing defects, such as fiber distortion, wrinkling, and tearing. In this study, we consider the development of two of these defects, namely wrinkling and tearing, in a press-formed dry plain woven glass fabric using a die-punch setup, and using finite element analysis, determine the forming limit of this fabric as a function of blank holder force and forming depth. It is shown that the punch corner radius has a critical role on the forming limit of the fabric.

Keywords: Fabric, forming limit diagrams, wrinkling, tearing, blank holder force, punch corner radius

1. Introduction

Fabric-reinforced composites are finding increasing applications in automotive body panels and structures, such as roof panels and B-pillars. The manufacturing process for these components using a thermosetting resin is called resin transfer molding that involves injection of a liquid resin into a dry fabric preform and curing the resin in place [1]. If a thermoplastic polymer is selected as the matrix, then the fabric is first embedded in the matrix, which is followed by press forming operation to make the composite part. One common method of preforming utilizes press forming operation in which a dry fabric or layers of dry fabric are placed on a preforming die and then shaped using a punch that pulls the fabric into the die. Depending on the press forming conditions used, fabric deformation characteristics and the die-punch design, several defects may form in the preformed fabric. Examples of these defects are fiber distortion, wrinkles and tearing. It will be useful if the parameters controlling the defect formation in fabrics can be predicted using a forming limit diagram (FLD) similar to the one used in the metal forming industry to predict the forming behavior of sheet metals.

Forming limit diagram for sheet metals is a graphical representation of the limit strains up to which a thin sheet blank can be shaped in different modes of deformation. The envelope formed by the boundary of the principal strains is called the forming limit curve (FLC). To avoid failure of the material it is necessary that the strain levels in the stamped part lie below the FLC [2-4]. Unlike sheet metals, forming limit studies for fabrics and fabric-reinforced composites have not been explored much. The process of developing FLC for sheet metals cannot be directly applied to fabric-reinforced composites, since the deformation in sheet metals during stamping takes place due to a combination of drawing and stretching, while the deformation in fabrics during press forming is primarily due to shear between the warp and weft yarns in the fabric. The fibers

in the yarns behave in an elastic manner and have low extensibility and low tensile strain-at-failure; as a result, there may be tearing if the tensile forces acting on them become too high. Furthermore, fabrics have low resistance to buckling and out-of-plane bending deformation.

Some of the defects which arise during press forming of fabrics are fiber distortion, wrinkling and tearing. Wrinkles can form when the fabric is draped over a die with highly curved shapes or corners with small radii that create shear and compressive stresses in the fabric. Since the fabric may not be able to adapt to the geometric form of the die [5], it results in the formation of wrinkles as shown in Figure 1. Wrinkling in this case has occurred due to buckling of the yarns at four locations on the hemispherical cup [6]. Wrinkles are also formed during press forming when the shear deformation between the warp and weft yarns in the fabric reaches a limit, known as shear locking. Until shear locking occurs, the yarns are able to slide on each other relatively easily. The shear stiffness of the fabric is mainly due to the friction between the yarns; however, at the onset of shear locking, the yarns are closely packed and any further increase in deformation leads to localized wrinkling due to low out-of-plane bending resistance of the fabric. With yarns now laterally compressed, there is further increase in shear stiffness of the fabric [7-8]. The other form of defects that are observed during press forming of fabrics is tearing. Tearing occurs when the tensile strain in the yarns of the fabric exceeds the ultimate strain-at-failure of the fibers.

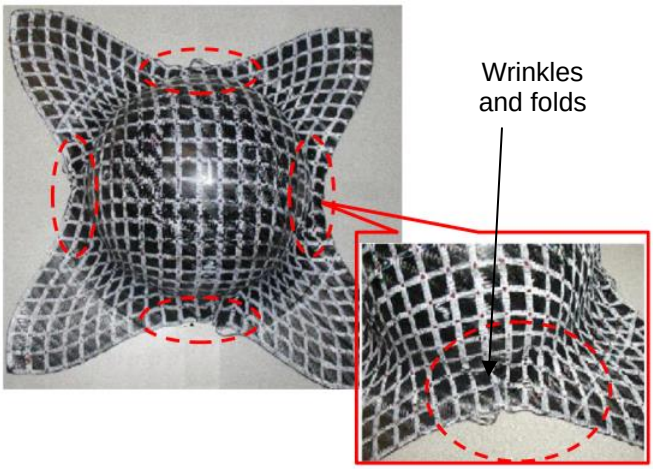

Figure 1. Wrinkle formation in the formed hemispherical cup of a fabric reinforced thermoplastic [6].

The concept of forming limit diagrams for composites was first introduced by Dessenberger and Tucker [9]. They used biaxial experiments it to develop FLD for a random fiber composite. There are also a couple of references [10-11] in which forming limit diagrams of fabric reinforced thermoplastic composites was developed by experiments to predict the onset of wrinkling in fabric-reinforced composites. The possibility of failure by tearing was not addressed in these references. The remaining available literature shows that the past research on this topic is concentrated principally on understanding the process conditions and the deformation mechanisms during press forming.

The objective of this study is to determine a safe window for press formability of a dry fabric layer using LS-DYNA, a non-linear finite element software used for forming analysis of metals as well as composites. The safe forming window, expressed as a function of blank holder force and forming depth, is determined by the ability of the fabric to form and retain the shape without generating wrinkles and tearing. The influence of the punch shape on the safe forming window is also studied.

2. Fabric and the press forming setup

The fabric under consideration in this study is ECK 12 which is a plain-woven glass fabric with the following properties: weft tow width = 2.18 ± 0.038 mm, warp tow width = 2.12 ± 0.052 mm, areal density = 311 g/m2, thickness = 0.206 ± 0.012 mm (product code = ECK12, Allscot) [12].

Figure 2 shows the die-punch setup used for finite element modeling of the press forming operation to produce a cup-shaped fabric preform. It consists of an open round die, a blank holder, and a punch. The die and punch materials are an aluminum alloy. The die opening radius is 40 mm and the punch radius is 38 mm so that the radial gap between the die wall and the punch is 2 mm. Four different punch bottoms were considered: (1) a hemispherical bottom with 38 mm radius, (2) a flat bottom with 15 mm corner radius, (3) a flat bottom with 5 mm corner radius, and (4) a flat bottom with sharp corner. The die corner radius was kept constant at 10 mm, which was selected based on the guidelines prescribed by Donaldson et al. [13] for metal forming applications. A punch velocity of 100 mm/s was selected for this study. To develop the forming limit window for the ECK 12 fabric, the blank holder force was varied between 0 and 80,000 N for each punch configuration and the forming depth corresponding to either wrinkling or tearing was obtained by simulation. A square fabric measuring 160 mm x160 mm was found suitable for the forming experiments using the mentioned die-punch setup.

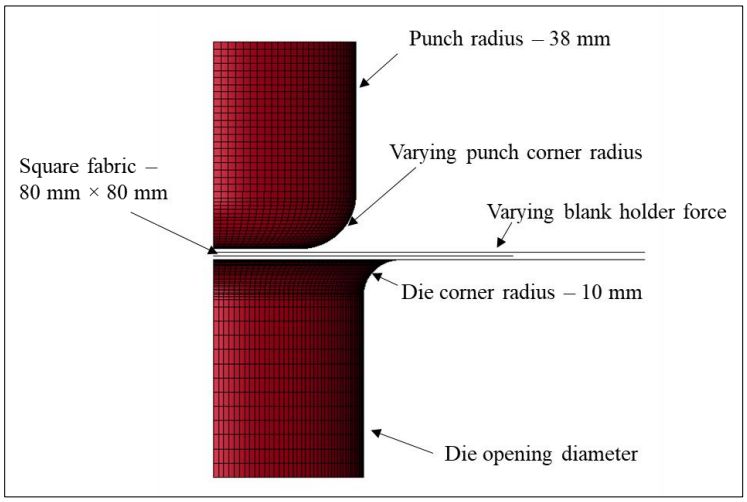

Figure 2. Press forming setup.

3. Numerical modeling

Material models available in LS-Dyna that are widely used to simulate the fabric deformation behavior during press forming operations include Viscoelastic loose fabric model (MAT_234), Micromechanics dry fabric model (MAT_235), and Anisotropic hyper-elastic model (MAT_249). These material models can successfully predict reorientation of the fabric yarns and simulate locking phenomenon [14]. To simulate press forming operation of a hemispherical dome shape, Yildirim and Ozturk [14] used these three material models and validated their modeling capabilities by comparing the simulated results with the experimental results. Their study shows that MAT_234 gives a more stable shear angle distribution and the outer contour of the simulated deep drawn cup shape matches well with the experimental shape.

In the current study, MAT_234 was selected to develop the forming limit diagram for dry fabrics. MAT_234 works with both reduced and fully integrated membrane elements [15]. For elements oriented at an angle with respect to the fiber direction, it is preferable to use under-integrated membrane elements. To use fully integrated membrane elements, the elements are to be oriented along the fiber direction to avoid tension locking [16]. Simulations with only membrane elements show multiple small wrinkles that are not observed experimentally [5, 17]. The reason for this can be attributed to the membrane elements not being able to include out-of-plane bending stiffness. Studies have shown that including out-of-plane bending stiffness even when they are very low compared to the tensile stiffness of the fabric will represent the true fabric deformation and play a key role in capturing the wrinkle onset, shape, and size [7, 18]. Different modeling approaches have been proposed [17, 19, 20, 21] that include in-plane shear behavior and out-of-plane bending stiffness for the fabrics so that they represent the true fabric deformation.

In the finite element models used here, the fabric ls represented by membrane elements superimposed with shell elements. The membrane elements account for the fabric's in-plane shear deformation and is assigned the material model MAT_234. The shell elements are used to account for the out-of-plane bending and are assigned the isotropic elastic material model MAT_001. The tensile modulus assigned to the shell elements can be obtained from the flexural stiffness of the fabric [20-21]. In the absence of the flexural stiffness of the fabric, the tensile modulus of the shell elements can be assigned a very small value, and it can be adjusted to match the experimental results. The membrane and shell elements are superimposed on one another. The duplicate nodes which arise due to the superimposition are merged so that they are mutually constrained and share the same nodes.

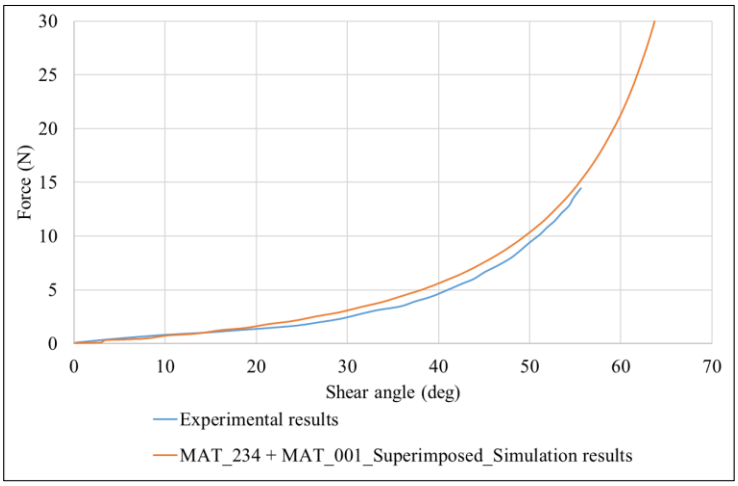

Figure 3. Comparison of uniaxial bias-extension test results of total force vs. shear angle by Harrison et al. [12] with the simulation results.

The modeling approach of superimposing membrane and shell elements and assigning a very low tensile modulus to the shell elements was used to verify if the superimposition approach can simulate the fabric deformation behavior observed in previously published results. Simulation results of uniaxial and biaxial bias-extension tests for ECK-12 plain woven glass fabric were validated with the experimental results of Harrison et al. [12]. The uniaxial bias-extension test is used for characterizing the shear deformation of fabrics and the biaxial bias-extension test is used

for characterizing the shear-tension coupling of fabric. Figures 3 and 4 show the comparison of the experimental and simulation results for uniaxial and biaxial bias extension tests respectively. It can be observed in these figures that the superimposition approach was able to capture the behavior of the ECK-12 fabrics determined experimentally.

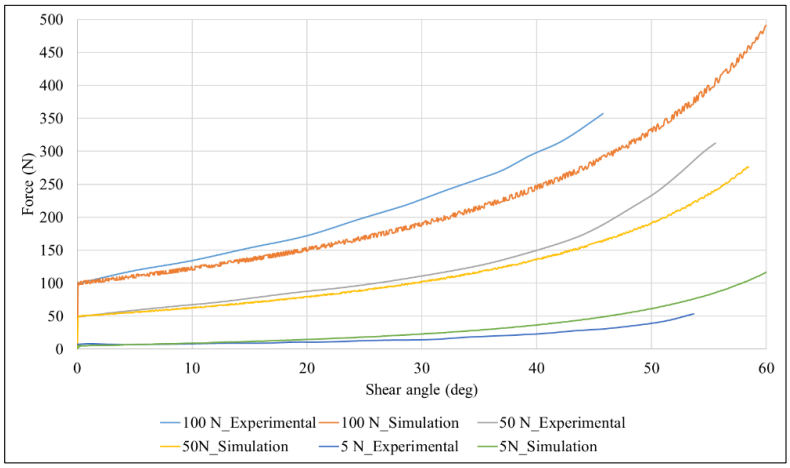

Figure 4. Comparison of biaxial bias-extension test results of total force vs. shear angle by Harrison et al. [12] with the simulation results.

4. Finite element modeling of fabric press forming

The finite element model in this study to develop the forming limit diagrams for ECK-12 plain woven glass fabrics is the same as that described in Section 3. The yarn orientation in the square fabric was 0/90, as was the element orientation. The mesh size for the die and the punch was selected to be 2 mm; however, a higher mesh density at both punch and die corner radii was used to accommodate the geometrical inconsistencies during press forming. The mesh size of the quadrilateral elements used for the fabric was selected as 1.5 mm. Because of symmetry, simulations were carried using a quarter model to achieve faster computational time. To represent the quarter model of the fabric, a square blank of 80 mm x 80 mm was used, and the necessary boundary conditions were applied. The total blank holder force was also divided by 4 to represent the quarter model.

To accommodate the in-plane shear properties of the fabric, the fabric was assigned to the reduced integrated membrane elements using MAT_234. The mechanical and the mesoscopic properties for ECK 12 plain glass fabric were kept the same as the parameters with which the bias extension simulations were carried out in Section 3. The ultimate strain at fiber failure for ECK-12 glass fabric is taken from literature as 4.8% [22]. To account for the out-of-plane bending stiffness, MAT_001 was assigned to the shell elements and a tensile modulus of 1.5 MPa that matched the experimental results of bias extension tests were used. The shell and membrane elements are superimposed on one another. Duplicate nodes which arise due to superimposition were merged to represent the fabric behavior. The aluminum die-punch set was modelled using rigid shell elements and material model MAT_020 (MAT_RIGID). Since the experimental data for the coefficient of friction between the warp and weft direction yarns of ECK 12 were not available, it was assumed to be 0.41 based on the recommendation by Yildrim et al. [14].

Three regions of contact were considered for this study: (a) contact between the punch and the blank, (b) contact between the blank holder and the blank, and (c) contact between the die and the blank. The coefficient of friction between aluminum and glass fabrics was selected as 0.2 based on the simulation results by Peng and Ding [23] who validated their results with experimental results and showed a correlation between the two using the friction co-efficient value of 0.2.

5. Results

Fabric press forming simulations on dry ECK 12 glass fabric were carried using LS-Dyna to study the variation of the successful forming depths (without wrinkling and tearing) with blank holder force and punch corner radius. For each punch corner radius considered, the blank holder force was varied, and the formed shape of the fabric was observed for any forming defects. The forming depth at which the defects were first observed was recorded and was used to plot the forming limit diagrams.

The following defects were observed during the dry fabric forming: (a) wrinkling due to yarn buckling at the intersections between the flanges, (b) wrinkling due to shear locking at the die entry radius and along the diagonals (Figure 5), (c) wrinkling at the punch corner radius, and (d) tearing of the fabric. These defects are shown in Figure 6. Tearing of the fabric was observed at very high blank holder forces when the strain in the yarns exceeded the ultimate strain-at-failure of the fibers. At lower blank holder forces, wrinkling observed in the formed fabric shape can be attributed to the compressive stresses at the locations shown in Figure 6 which later resulted in the formation of folds. With the increase in blank holder force, the wrinkles due to compressive stresses were reduced as can be seen in Figure 7 and only the wrinkles due to shear locking were observed. Wrinkles due to shear locking were observed at almost the same forming depth irrespective of the blank holder force. This can be attributed to the dry fabric conforming to the shape of the die corner radius and to the shear deformation as the fabric passed over the die corner radius. Wrinkles were also observed at the cup bottom when the punch with very sharp corner radius was used; however, these wrinkles were reduced with increase in the punch corner radius.

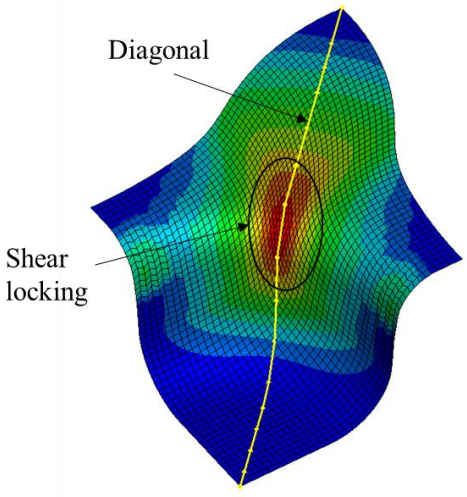

Figure 5. Wrinkling due to shear locking (15 mm punch corner radius, 37 mm forming depth)

The recorded forming depths without any defects at different blank holder forces and for various punch corner radii were utilized to determine the safe forming windows for the ECK-12 glass fabric shown in Figure 8 (a-d). The region to the left side of these figures represents the safe forming window for fabrics, whereas the region to the top right represents the tearing behavior and the region in the bottom right represents the wrinkling behavior. The dashed line marks the transition between wrinkling and tearing; below the dashed line wrinkling defects were observed on the formed fabric which at higher blank holder forces ultimately led to tearing defects. Blank holder forces shown in Figure 8 are the values for the full model.

As can be seen in Figure 8, the safe forming window decreases with decrease in punch corner radius. With the increase in blank holder force the safe window initially increases which can be attributed to reduction in the formation of wrinkles due to yarn buckling with applied load, however at high loads, tearing defects were observed in the formed fabric which in turn reduces the formability window.

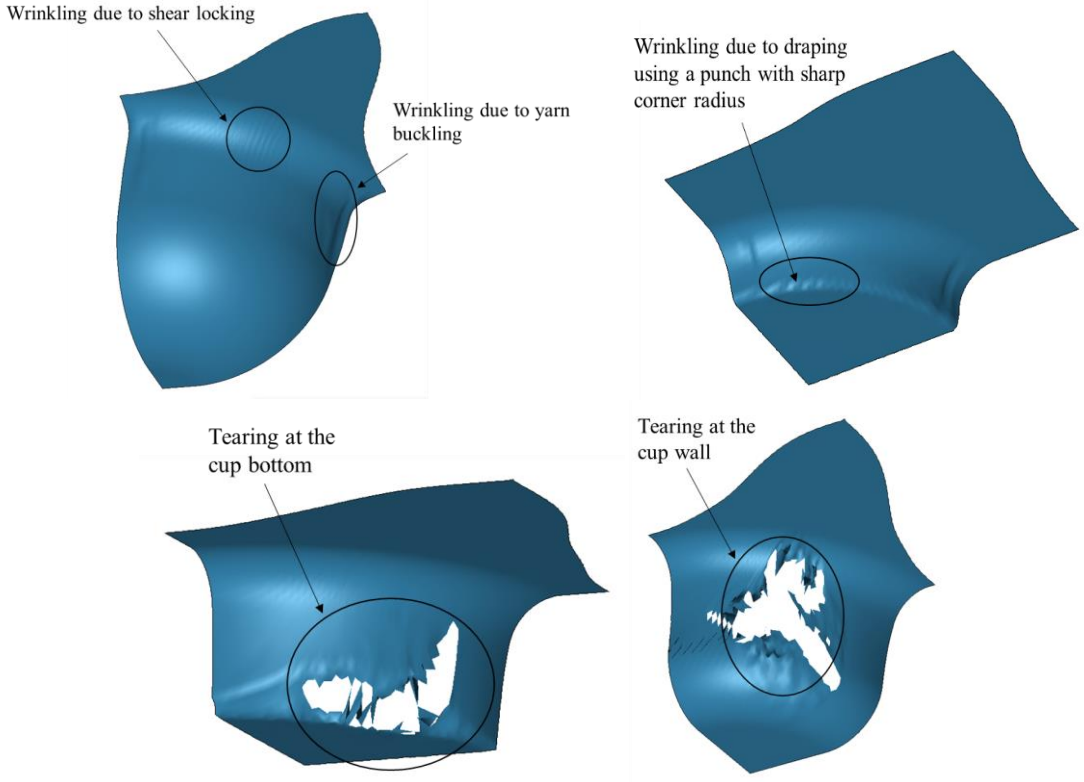

Figure 6. Defects observed during dry fabric forming: (a) wrinkling due to yarn buckling (0 mm punch corner radius), (b) wrinkling due to shear locking (0 mm punch corner radius), (c) wrinkling at the cup bottom (0 mm punch corner radius), (d) tearing at the cup bottom (0 mm punch corner radius), (e) tearing at the cup wall (15 mm punch corner radius)

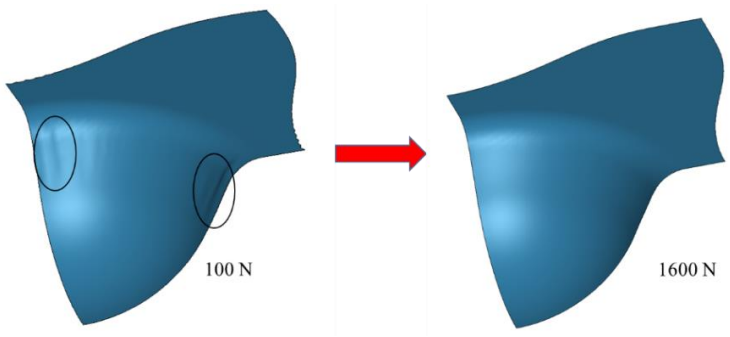

Figure 7. Reduction of wrinkles due to yarn buckling with increase in blank holder force from 100 N to 1600 N (with hemispherical punch bottom of radius 38 mm and at 40 mm forming depth).

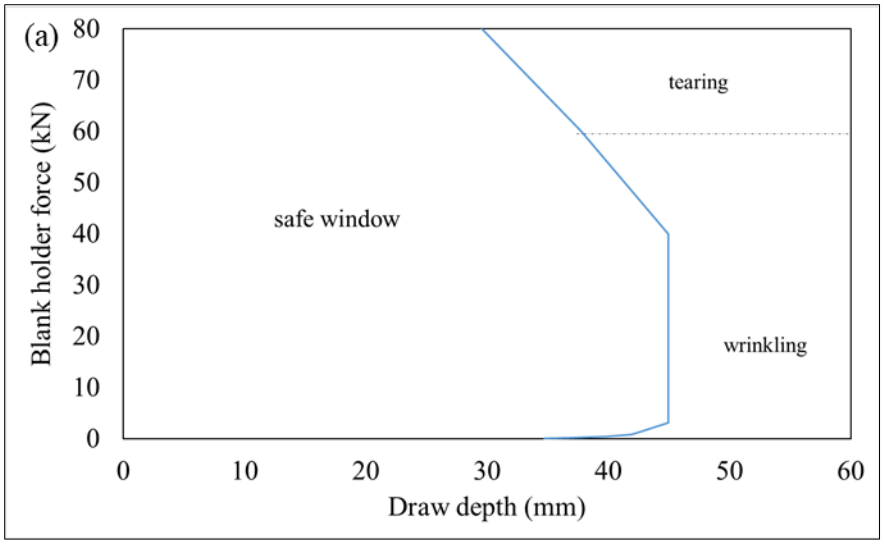

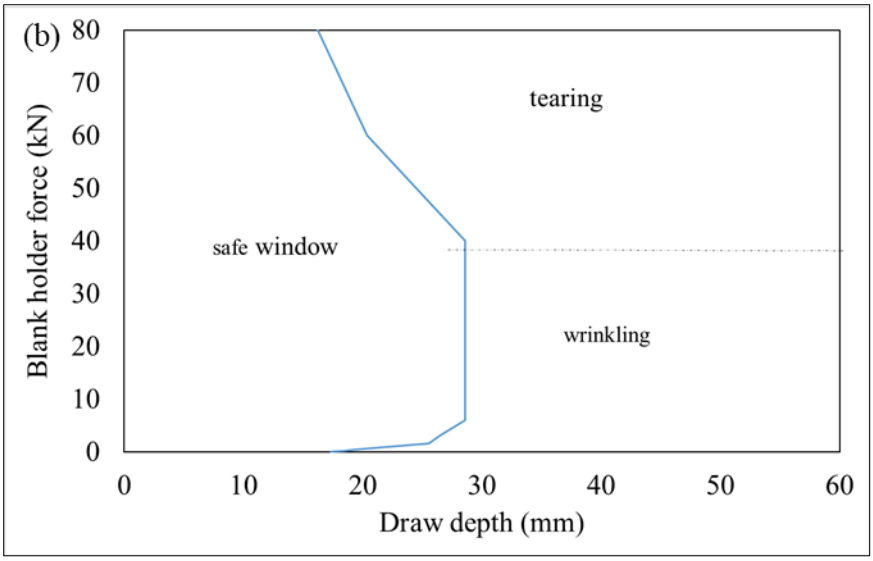

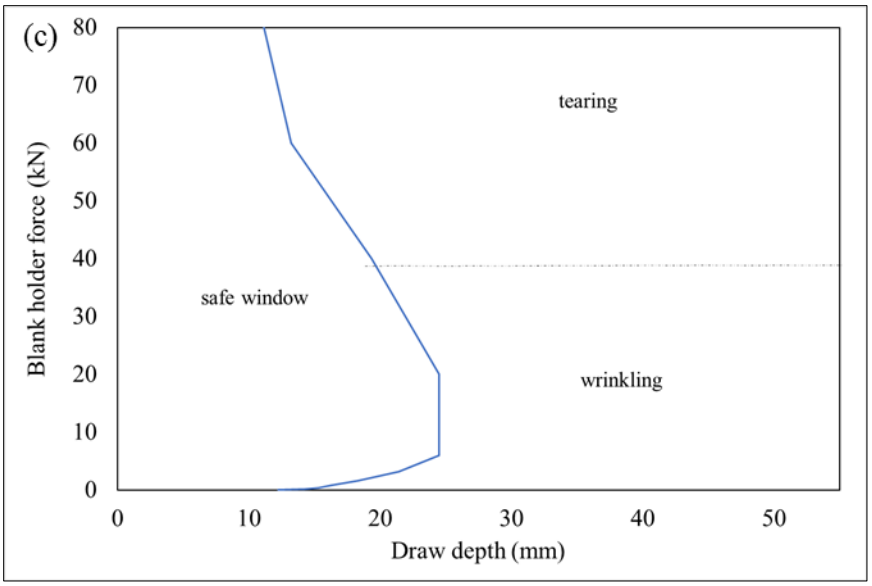

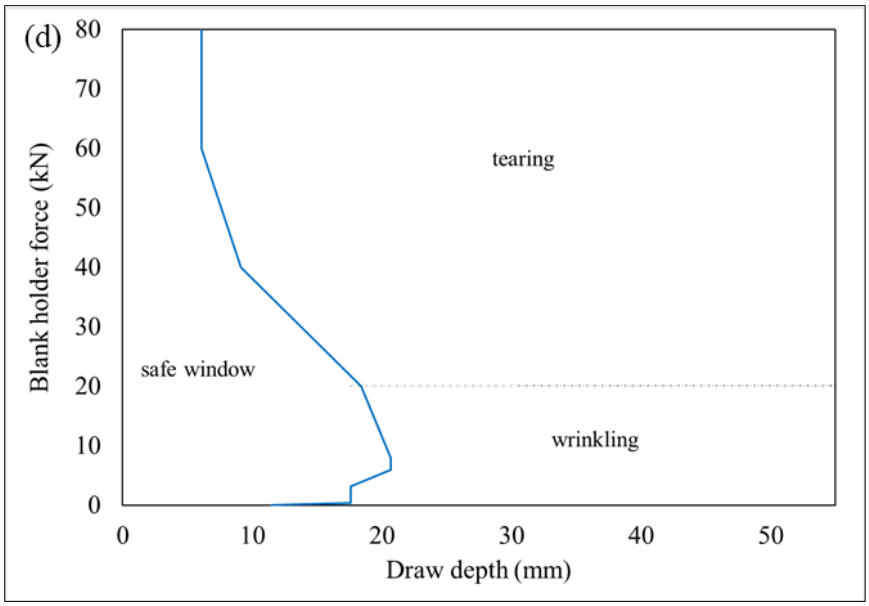

Figure 8. Safe forming window: (a) 38 mm punch corner radius (hemispherical punch), (b) 15 mm punch corner radius, (c) 5 mm punch corner radius, and (d) 0 mm punch corner radius.

The outer shape contours of one quarter of the press formed fabric at 40 mm and 55 mm forming depths for 38 mm punch corner radius are shown in Figure 9. It can be observed in this figure that there was little or no difference of the shape contours at 40 mm forming depth, however the wrinkle formation and the outer shape contours showed significant variation at 55 mm forming depth. At 55 mm forming depth, the shape contour with 100 N blank holder force was different from the shape contours with the other blank holder forces. Above 400 N blank holder force, the outer contour was almost the same with the other blank holder forces. Thus, these observations show that the effect of the blank holder force on the final shape formation is reduced above a limiting value, which for this fabric and with these forming parameters was 400N; however, the blank holder force has a significant role on the formation of wrinkles and tearing.

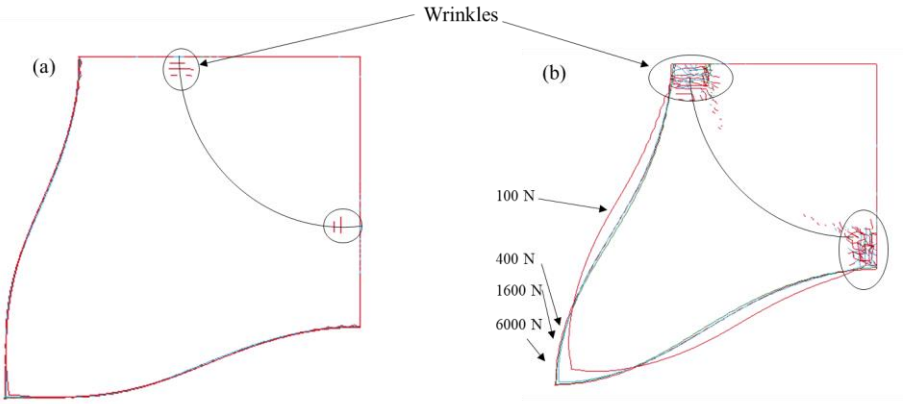

Figure 9. Flange shape contours shown for the quarter model of the press formed fabric as viewed from the top at (a) 40 mm, (b) 55 mm punch displacements with 100, 400, 1600 and 6000 N applied blank holder forces.

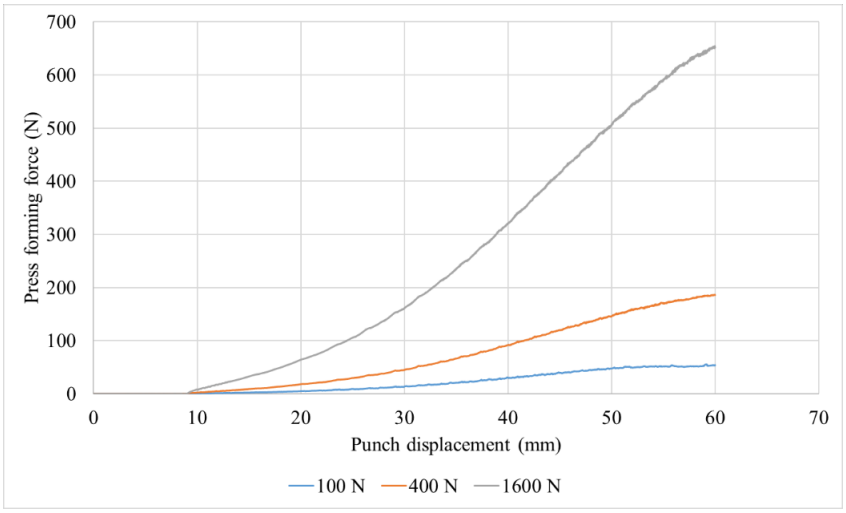

Figure 10. Press forming force vs. punch displacement at 100, 400 and 1600 N blank holder forces.

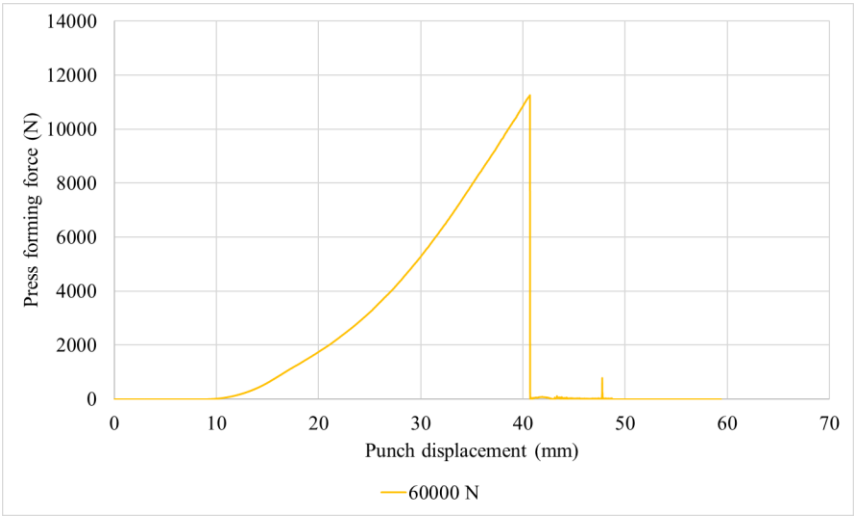

Figure 11. Press forming force vs. punch displacement at 60 kN blank holder force.

Figure 10 shows the plots of press forming force vs. punch displacement at 100 N, 400 N and 1600 N blank holder forces. As anticipated, the press forming force required for preforming the fabric increases with increasing blank holder force. In Figure 11, the press forming force was plotted at a high blank holder force of 60 kN. Sudden drop in the press forming force indicates tearing of the fabric which occurred when the tensile strain in the yarns of the fabric exceeded the ultimate strain-at-failure for the fibers at a punch displacement of 37.78 mm.

6. Conclusions

Based on the study for the development of a formability window for dry fabrics the following conclusions can be made.

At lower blank holder forces, wrinkles are observed at the intersections between the flanges due to yarn buckling. With increase in blank holder force, wrinkles due to compressive stresses are reduced. Wrinkles are also formed due to shear locking at the die entry radius along the diagonals of the square fabric specimen and when a punch with a sharp corner radius is used. When the fabric is pulled over the die corner radius, shear deformation occurs in the fabric and as the forming depth is increased, wrinkles start to appear in the fabric due to shear locking phenomenon. Wrinkle formation due to shear locking does not appear to depend on the blank holder force. Increasing the punch corner radius reduces the formation of wrinkles at the cup bottom. Hence, an optimum punch radius must be selected while press forming fabrics to avoid wrinkle formation at the cup bottom.

The forming limit diagrams for fabrics in which a safe forming window is expressed as a function of blank holder force and punch corner radius gives the limits for press forming fabrics. The safe forming window decreases with decrease in the punch corner radius, and with the applied blank holder force, the forming window increases initially due to a reduction of wrinkles formed due to compressive stresses. However, at higher blank holder forces the safe window again decreases with the applied load as the fiber strain in the yarns of the press formed fabric exceeds the ultimate strain-at-failure of the fibers.

This study was done to develop the forming limit diagram of a dry fabric. A similar study is being conducted to develop the forming limit diagrams of a fabric-reinforced polypropylene, which is a thermoplastic polymer widely used for automotive applications. The finite element model for this study will include not only superimposed elements to represent the fabric deformation, but also a non-linear material model developed specifically to represent the deformation of the polypropylene matrix.

References

[1] P. K. Mallick, Processing of Polymer Matric Composites, Boca Raton: FL:CRC Press: Taylor & Francis Group, 2018.

[2] S. Holmberg, B. Enquist and P. Thilderkvist, "Evalutaion of sheet metal formability by tensile tests," *Journal of Material Processing Technology,* vol. 145, no. 1, pp. 72-83, 2004.

[3] S. Kumar, T. Amjith and C. Anjaneyulu, "Forming limit diagram generation of Aluminum alloy of AA2014 using Nakazima test simulation tool," *Procedia technology,* vol. 24, pp. 386-393, 2016.

[4] S. P. Keeler, "Determination of forming limits in automotive stamping," *SAE tehcnical paper series 650535,* 1965.

[5] R. Azzouz, S. Allaoui and R. Moulart, "Composite preforming defects: a review and a classification," *International Journal of Material Forming,* vol. 14, no. 6, pp. 1259-1278, 2021.

[6] A. Skordos, C. Monroy Aceves and M. Sutcliffe, "A simplified rate dependent model of forming and wrinkling of pre-impregnated woven composites," *Composites Part A: Applied Science and Manufacturing,* vol. 38, no. 5, pp. 1318-1330, 2007.

[7] P. Boisse, N. Hamila and E. Vidal-Salle, "Simulation of wrinkling during textile composite reinforcement forming. Influence of tensile, in-plane shear and bending stiffnesses," *Composites Science and Technology,* vol. 71, no. 5, pp. 683-692, 2011.

[8] W. Lee, "Bias-extension of woven fabrics," *International Journal of Material Forming,* vol. 1, no. 1, pp. 895-898, 2008.

[9] R. Dessenberger and C. L. Tucker III, "Forming limit measurements for random fiber mats," *Polymer composites,* vol. 19, no. 4, pp. 370-376, 1998.

[10] V. Viisainen, J. Zhou and M. P. Sutcliffe, "Development of a composite forming diagram: A feasibility study," in *22nd Internatiional Conference on Composite Materials*, Melbourne, Australia, Aug 2019.

[11] K. Vanclooster, S. V. Lomov, I. Verpost and , "On the formability of muti-layered fabric composites," in *ICCM Inernational Conferences on Composite Materials*, Edinburgh, Scotland, 2009.

[12] P. Harrison, F. Abdiwi, Z. Guo, P. Potluri and W. R. Yu, "Characterising the shear–tension coupling and wrinkling behaviour of woven engineering fabrics," *Composites. Part A, Applied Science and Manufacturing,* vol. 43, no. 6, pp. 903-914, 2012.

[13] C. Donaldson, G. H. LeCain and V. C. Goold, Tool Design (3rd ed.), New York: McGraw-Hill, 1973.

[14] H. Yildirim and F. Ozturk, "A benchmark study of the material models for forming simulation of woven fabrics," *Journal of the Textile Institute,* pp. 1-12, 2021.

[15] A. Tabiei and I. Ivanov, "Computational micro-mechanical model of flexible woven fabric for finite element impact simulation," *International Journal for Numerical Methods in Engineering,* vol. 53, no. 6, pp. 1259-1276, 2002.

[16] N. Hamila and P. Boisse, "Locking in simulation of composite reinforcement deformation. Analysis and treatment," *Composite. Part A, Applied science and Manufacturing,* vol. 53, pp. 109-117, 2013.

[17] M. Nishi and T. Hirashima, "Approach for dry textile composite forming simulation," *International Conference on Composite Materials,* pp. 7486-7493, 2013.

[18] B. Liang, N. Hamila, M. Peillon and P. Boisse, "Analysis of thermoplastic prepreg bending stiffness during manufacturing and of its influence on wrinkling simulations. Composites," *Part A, Applied Science and Manufacturing,* vol. 67, pp. 111-122, 2014.

[19] D. Jauffres, C. Morris and J. Sherwood, "Discrete mesoscopic modeling for the simulation of woven-fabric reinforcement forming," *Internation Journal of Material Forming,* vol. 3, no. 2, pp. 1205-1216, 2010.

[20] P. Harrison, "Modelling the forming mechanics of engineering fabrics using a mutually constrained pantographic beam and membrane mesh," *Composites. Part A, Applied Science and Manufacturing,* vol. 81, pp. 145-157, 2016.

[21] A. J. Thompson, J. P. Belnoue and S. R. Hallett, "Modelling defect formation in textiles during the double diaphragm forming process," *Composites. Part B, Engineering,* vol. 202, p. 108357, 2020.

[22] P. K. Mallick, Fiber-Reinforced Composites: Materials, Manufacturing, and Design, Bosa Roca: CRC Press, 2007.

[23] X. Peng and F. Ding, "Validation of a non-orhtogonal constitutive model for woven composite fabrics via hemispherical stamping simulation," *Composite Part A: Applied Science and Manufacturing,* vol. 42, no. 4, pp. 400-407, 2011.